

Inhomogeneous Shadowing Effects on J/ψ Production in dA Collisions

S. R. Klein¹ and R. Vogt^{1,2}

¹*Nuclear Science Division, Lawrence Berkeley National Laboratory, Berkeley, CA 94720, USA*

²*Physics Department, University of California, Davis, CA 95616, USA*

Abstract

We study the effect of spatially homogeneous and inhomogeneous shadowing on J/ψ production in deuterium-nucleus collisions. We discuss how the shadowing and its spatial dependence may be measured by comparing central and peripheral dA collisions. These event classes may be selected by using gray protons from heavy ion breakup and events where the proton or neutron in the deuterium does not interact. We find that inhomogeneous shadowing has a significant effect on central dA collisions, larger than is observed in central AA collisions. The inhomogeneity may be measured by comparing the rapidity dependence of J/ψ production in central and peripheral collisions. Results are presented for dAu collisions at $\sqrt{s_{NN}} = 200$ GeV and dPb collisions at $\sqrt{s_{NN}} = 6.2$ TeV.

I. INTRODUCTION

The nuclear quark and antiquark distributions have been probed through deep inelastic scattering (DIS) of leptons and neutrinos from nuclei. These experiments showed that parton densities in free protons are modified when bound in the nucleus [1]. This modification, referred to collectively as shadowing, depends on the parton momentum fraction x and the square of the momentum transfer, Q^2 . Most models of shadowing predict that the modification should vary depending on position within the nucleus [2]. Most DIS experiments have been insensitive to this position dependence. However, some spatial inhomogeneity has been observed in νN scattering in emulsion [3].

Deuterium-nucleus collisions at heavy ion colliders offer a way to measure the structure functions of heavy nuclei at higher energies, and hence lower x and higher Q^2 than are currently possible with fixed target DIS experiments. In addition, dA collisions are more sensitive to the gluon distributions in nuclei than DIS. These dA collisions are preferred over pA collisions for technical reasons - the two beams have similar charge Z to mass A ratios, simplifying the magnetic optics. Several groups have previously considered structure function measurements using pA and dA collisions. However, the spatial dependence has not yet been explored. A measurement of the spatial dependence would be of great interest

both as a probe of the shadowing mechanism and as an important input to studies of AA collisions.

In this letter, we show that dA collisions can be used to study the spatial dependence of nuclear gluon shadowing. We consider two concrete examples: dAu interactions at $\sqrt{s_{NN}} = 200$ GeV at RHIC and 6.2 TeV dPb interactions at the LHC. The RHIC conditions correspond to the Spring, 2003 run.

We choose the J/ψ as a specific example since it has already been observed in pp and $Au+Au$ interactions at RHIC [4]. Since we wish to focus on the magnitude of the shadowing effect, we do not include nuclear absorption or transverse momentum, p_T , broadening in our calculations. The techniques and general conclusions that we discuss should be equally applicable to other hard probes such as Υ , open charm and bottom quarks, Drell-Yan dileptons, jets, and dijets. At the LHC, similar approaches should also apply for W^\pm and Z^0 production. By using a variety of probes, both quark and gluon shadowing can be measured over a wide range of x and Q^2 .

Our J/ψ calculations employ the color evaporation model (CEM) which treats all charmonium production identically to $c\bar{c}$ production below the $D\bar{D}$ threshold, neglecting the color and spin of the produced $c\bar{c}$ pair. The leading order (LO) rapidity distributions of J/ψ 's produced in dA collisions at impact parameter b is

$$\frac{d\sigma}{dyd^2bd^2r} = 2F_{J/\psi}K_{\text{th}} \int dz dz' \int_{2m_c}^{2m_D} M dM \left\{ F_g^d(x_1, Q^2, \vec{r}, z) F_g^A(x_2, Q^2, \vec{b} - \vec{r}, z') \frac{\sigma_{gg}(Q^2)}{M^2} \right. \\ \left. + \sum_{q=u,d,s} [F_q^d(x_1, Q^2, \vec{r}, z) F_q^A(x_2, Q^2, \vec{b} - \vec{r}, z') + F_q^d(x_1, Q^2, \vec{r}, z) F_q^A(x_2, Q^2, \vec{b} - \vec{r}, z')] \frac{\sigma_{q\bar{q}}(Q^2)}{M^2} \right\}. \quad (1)$$

The LO partonic $c\bar{c}$ cross sections are defined in Ref. [5], $M^2 = x_1 x_2 s$ and $x_{1,2} = (M/\sqrt{s_{NN}}) \exp(\pm y) \approx (m_{J/\psi}/\sqrt{s_{NN}}) \exp(\pm y)$ where $m_{J/\psi}$ is the J/ψ mass. The fraction of $c\bar{c}$ pairs below the $D\bar{D}$ threshold that become J/ψ 's, $F_{J/\psi}$, is fixed at next-to-leading order (NLO) [6]. Both this fraction and the theoretical K factor, K_{th} , drop out of the ratios. We use $m_c = 1.2$ GeV and $Q = M$ [6].

We assume that the nuclear parton densities, F_i^A , are the product of the nucleon density in the nucleus $\rho_A(s)$, the nucleon parton density $f_i^N(x, Q^2)$, and a shadowing function $S_{P,S}^i(A, x, Q^2, \vec{r}, z)$ where \vec{r} and z are the transverse and longitudinal location of the parton in position space with $s = \sqrt{r^2 + z^2}$ and $s' = \sqrt{|\vec{b} - \vec{r}|^2 + z'^2}$. The first subscript, P, refers to the choice of shadowing parameterization, while the second, S, refers to the spatial dependence. All available shadowing parameterizations ignore effects in deuterium. However, we take the proton and neutron numbers of both nuclei into account. Thus,

$$F_i^d(x, Q^2, \vec{r}, z) = \rho_d(s) f_i^N(x, Q^2) \quad (2)$$

$$F_j^A(x, Q^2, \vec{b} - \vec{r}, z') = \rho_A(s') S_{P,S}^j(A, x, Q^2, \vec{b} - \vec{r}, z') f_j^N(x, Q^2). \quad (3)$$

In the absence of nuclear modifications, $S_{P,S}^i(A, x, Q^2, \vec{r}, z) \equiv 1$. The nucleon densities of the heavy nucleus are assumed to be Woods-Saxon distributions based on measurements of the nuclear charge distributions with $R_{Au} = 6.38$ fm and $R_{Pb} = 6.62$ fm [7]. The deuteron wave function is predominantly S wave with a small D wave admixture. We use the Hulthen wave function [8] to calculate the deuteron density distribution. The central densities are

normalized so that $\int d^2r dz \rho_A(s) = A$. We employ the MRST LO parton densities [9] for the free nucleon.

We have chosen two recent parameterizations of the nuclear shadowing effect which cover extremes of gluon shadowing at low x . The Eskola *et al.* parameterization, EKS98, is based on the GRV LO [10] parton densities. Valence quark shadowing is identical for u and d quarks. Likewise, the shadowing of \bar{u} and \bar{d} quarks are identical. Shadowing of the heavier flavor sea, \bar{s} and higher, is calculated separately. The shadowing ratios for each parton type are evolved to LO for $1.5 < Q < 100$ GeV and are valid for $x \geq 10^{-6}$ [11,12]. Interpolation in nuclear mass number allows results to be obtained for any input A . The parameterization by Frankfurt, Guzey and Strikman, denoted FGS here, combines Gribov theory with hard diffraction [13]. It is based on the CTEQ5M [14] parton densities and evolves each parton species separately to NLO for $2 < Q < 100$ GeV. Although the given x range is $10^{-5} < x < 0.95$, the sea quark and gluon ratios are unity for $x > 0.2$. The EKS98 valence quark shadowing ratios are used as input since Gribov theory does not predict valence shadowing. The parameterization is available for four different values of A : 16, 40, 110 and 206. We therefore use the FGS parameterization for $A = 206$ with both Au and Pb.

Figure 1 compares the homogeneous ratios, S_{EKS98} and S_{FGS} for $Q = 2m_c$. The FGS calculation predicts far more shadowing at small x . The difference is especially large for gluons. The FGS approach thus predicts larger antishadowing at $x \sim 0.1$. The valence and sea ratios are also shown, for completeness.

We have calculated homogeneous shadowing effects on J/ψ production at NLO. However, the additional integrals required to calculate inhomogeneous effects at NLO lead to significant numerical difficulties. Therefore we have compared the LO and NLO calculations of homogeneous shadowing in $p\text{Au}$ interactions at $\sqrt{s_{NN}} = 200$ GeV using the EKS98 parameterization to verify that the results are essentially identical.

Some differences may arise from the use of the MRST HO [15] parton densities in the NLO code while the LO calculation uses the MRST LO [9] parton densities. In addition, at NLO, a new production channel, qg scattering, also contributes. However, its contribution is small. The NLO and LO ratios agree well because J/ψ production is dominated by gluons for $x_F < 0.6$. Thus the gg channel is dominant for $|y| < 3$ at RHIC and $|y| < 6.4$ at the LHC and the LO calculation should reproduce the essential effects of inhomogeneous shadowing.

Shadowing is not the only nuclear effect on J/ψ production. Broadening of the p_T distributions, observed in fixed-target measurements [16], arises from multiple scattering of the initial-state partons [17] and does not affect the total cross section. Thus, a p_T -integrated measurement should be insensitive to this effect. Nucleon absorption depends on the J/ψ production mechanism [18]. Absorption is generally expected to increase at large negative rapidities where the J/ψ may hadronize inside the target. However, this regime is reached outside the rapidity coverage of the present detector configurations.

We now turn to the spatial dependence of the shadowing. Since the data are limited, we use parameterizations of the spatial dependence. We compare two parameterizations that we have used for inhomogeneous shadowing in AA collisions [2,19–21]. The first, $S_{\text{P,WS}}$, assumes that shadowing is proportional to the local density, $\rho(s)$,

$$S_{\text{P,WS}}^i(A, x, Q^2, \vec{r}, z) = 1 + N_{\text{WS}}[S_{\text{P}}^i(A, x, Q^2) - 1] \frac{\rho_A(s)}{\rho_0}, \quad (4)$$

where ρ_0 is the central density and N_{WS} is chosen so that $(1/A) \int d^2r dz \rho_A(s) S_{\text{P,WS}}^i = S_{\text{P}}^i$. When $r \gg R_A$, the nucleons behave as free particles while in the center of the nucleus, the modifications are larger than the average value S_{P}^i .

If, on the other hand, shadowing stems from multiple interactions of the incident parton [22], parton-parton interactions are spread longitudinally over the coherence length, $l_c = 1/2m_N x$, where m_N is the nucleon mass [23]. For $x < 0.016$, $l_c > R_A$ for any A . The interaction is then delocalized over the entire trajectory so that the incident parton interacts coherently with all the target partons along its path length. At large x , $l_c \ll R_A$ and shadowing is proportional to the local density, as above. In practice, the numerical differences between the two models are small and the available data [3] is inadequate to tell the difference. However, the both models predict significant differences with the homogenous shadowing that is usually used.

Because of the difficulty of matching the shadowing at large and small x while conserving baryon number and momentum, we consider the small x and large x limits separately. This matching is necessary because, for $y < -2$ at RHIC, $l_c < R_{\text{Au}}$. This regime is measurable in the PHENIX muon spectrometers [4]. Equation (4) corresponds to the large x limit. When $l_c \gg R_A$, the spatial dependence may be parameterized as

$$S_{\text{P},\rho}^i(A, x, Q^2, \vec{r}, z) = 1 + N_\rho (S_{\text{P}}^i(A, x, Q^2) - 1) \frac{\int dz \rho_A(\vec{r}, z)}{\int dz \rho_A(0, z)}. \quad (5)$$

The integral over z includes the material traversed by the incident nucleon. The normalization requires $(1/A) \int d^2r dz \rho_A(s) S_{\text{P},\rho}^i = S_{\text{P}}^i$. We find $N_\rho > N_{\text{WS}}$.

Figures 2 and 3 show the ratios of J/ψ production per nucleon in dA interactions with and without shadowing as a function of rapidity at RHIC ($\sqrt{s_{NN}} = 200$ GeV) and the LHC ($\sqrt{s_{NN}} = 6.2$ TeV). These ratios are essentially equivalent to the dA per nucleon to pp ratio at the same energy since isospin has a negligible effect on J/ψ production.

We consider three cases: central collisions, $b < 0.2R_A$, peripheral collisions, $0.9R_A < b < 1.1R_A$, and minimum-bias interactions, covering all b . Central collisions can be selected by choosing events with a large number of ‘grey protons’ which move with approximately the beam rapidity. Grey protons, slow in the target rest frame, are ejected from the heavy nucleus in the collision. The name originates from the appearance of their tracks in nuclear emulsion. Their momentum must be larger than the Fermi momentum of the target. The number of grey protons is related to the number of individual NN collisions, ν , which is closely related to the impact parameter. Thus the number of grey protons could be used to select quite central collisions. This technique was used in the νA study of inhomogeneity [3] as well as in lower energy pA studies [24]. In the multiple interaction picture, shadowing should be directly proportional to ν .

At a heavy ion collider, grey protons can be detected in a forward proton calorimeter (FPC). Neutrons detected in a zero degree calorimeter (ZDC), could also be used, although, because of the transverse momentum, the acceptance would be limited.

The number of NN collisions is larger in dA than in pA interactions, reducing the uncertainty in the impact parameter determination. In a large acceptance detector, it might also be possible to use total multiplicity to enhance the impact parameter determination.

Peripheral collisions could be selected using two criteria. Selecting events with a small number of grey protons preferentially chooses a small number of interactions. It is also

possible to select events where only one of the nucleons in the deuteron interacts while the other is unaffected. Non-interacting neutrons can be detected in a ZDC while non-interacting protons could be seen in a FPC. In these NA collisions, the interacting deuterium nucleon is usually near the surface of the heavy ion, so that $b > R_A - 2$ fm. However, since the deuteron has a significant density even at large distances, not all single-nucleon interactions are very peripheral.

A complication for dA collisions is that the difference between one or two deuterium participants in the interaction is significant. This complication can be partly controlled by detecting the non-interacting nucleon in forward calorimeters. It can be further controlled by studying the J/ψ rapidity distribution. The rapidity, $y = y_c$, at which shadowing disappears, $S_p^i \rightarrow 1$, could be used as a calibration point. If the deuterium comes from negative rapidity, J/ψ production at negative y occurs via small x partons in the deuteron. The rapidity distribution ratios are essentially mirror images of the shadowing parameterizations in Fig. 1. Since $S_p^g \approx 1$ at $x \approx 0.025$, $y_c \approx -0.2$ at RHIC and -3.2 at the LHC.

The J/ψ rate at $y = y_c$ could be used to normalize the cross sections in different impact parameter classes, necessary if the absolute efficiency of cuts on grey protons is difficult to assess. Note that $y > y_c$ corresponds to low x in the heavy nucleus while at $y < y_c$, the antishadowing region is entered. The point $y = y_c$ could also be used to normalize the dA data to pp data at the same energy, allowing a direct measurement of shadowing since higher order corrections unrelated to shadowing cancel out in the ratio. Although y_c may not be perfectly known, the exact value of y_c is not important since a slight error will only affect the absolute values of the ratio. Another advantage to this normalization is that, if, as expected, the J/ψ absorption is independent of rapidity in the region of interest, any impact parameter dependence in the absorption correction will drop out.

The homogeneous results are indicated by the solid (EKS98) and dashed (FGS) lines. The local density approximation of inhomogeneous shadowing is shown by the circles and squares while the path length approximation is shown by the x's and diamonds. It is obvious that $S_{p,\rho}^i$ has a stronger spatial dependence.

In central collisions, the inhomogeneous shadowing is stronger. The stronger the homogeneous shadowing, the larger the effect of the spatial dependence. In peripheral collisions, the inhomogeneous effects are somewhat weaker than the homogeneous results but some shadowing is still present. Shadowing persists in part because the density in a heavy nucleus is large and approximately constant except close to the surface and partly because the deuteron wave function has a non-zero amplitude at quite large distances. Due to these tails, we expect some shadowing effects even at very large impact parameters where there are almost no interactions. Figures 2(c) and 3(c) show that the impact parameter integrated results are identical to the homogeneous results, as expected.

In dA collisions, the rapidity-dependent inhomogeneity is somewhat stronger than that predicted for AA collisions [2]. Central dA collisions are confined to the center of the target nucleus, where the effect is stronger, while central AA collisions include both central and peripheral nucleon-nucleon interactions.

The predicted spatial dependence would be even stronger for proton projectiles than for deuterons since the proton is effectively a point particle in this approach. In contrast, the deuteron is the same size, $r \approx 2$ fm, as an intermediate mass nucleus. However, it would be considerably more difficult to determine the impact parameter in pA collisions since the

number of grey protons is reduced and no spectator nucleon would be left on the proton side. In fact, light ion projectiles may offer an attractive combination, with enough interactions for an accurate impact parameter measurement, but little projectile shadowing.

It should be possible to measure shadowing at midrapidity at RHIC, particularly if the gluon shadowing is strong, as with the FGS parameterization. However, measurements at high $|y|$ could prove more insightful, as seen in Fig. 2. At RHIC, measurements have been made in pp , dAu and $Au+Au$ at the same $\sqrt{s_{NN}}$, allowing direct comparison. The STAR electromagnetic calorimeter [25] covers $-2 < \eta < 1$, encompassing part of the antishadowing and shadowing regions. The PHENIX muon arms [4] cover $1 \leq |y| \leq 2.4$ and could measure the low and high x regions while the PHENIX electron spectrometers, $|y| \leq 0.35$, cover the region near y_c . It would then be possible to compare the antishadowing region, $y \sim -2$ with the shadowing region, $y \sim 2$. Both detectors should be able to study most of the J/ψ p_T spectrum. A cut on minimum lepton p_T might reduce the sensitivity to low p_T J/ψ s. A cut on J/ψ p_T would increase the x and Q^2 values probed at a given y , allowing cross-checks on the shadowing data. The ‘cost’ of this cut would be some sensitivity to p_T broadening.

The higher energy of the LHC moves the antishadowing region out of the reach of any planned lepton coverage. Only the low x and transition regions might be observable at low p_T , see Fig. 3. Both the central detectors of ALICE [26] ($|y| \leq 0.9$) and CMS [27] ($|y| \leq 2.4$ for the central and forward arms) should be able to clearly distinguish both the homogeneous effect and the gross features of the inhomogeneity. The ALICE forward muon spectrometer [28], $2.5 \leq y \leq 4$, could probe the lowest and highest x values possible at the LHC, if both dA and Ad collisions were studied. A p_T cut on the J/ψ would increase the x and Q^2 values, perhaps moving the antishadowing region within reach. The Υ has a very similar production mechanism, but would probe larger x and Q^2 values, and should thus be sensitive to antishadowing at large $|y|$.

In conclusion, we have shown how nuclear shadowing can be measured with J/ψ production in dA collisions. The J/ψ rapidity is related to the momentum fraction of the target parton, allowing for measurement of the x dependence of shadowing. By selecting events with different numbers of grey protons and/or a surviving spectator nucleon from the deuteron, it is possible to study the spatial dependence of shadowing. In all of the models considered, the spatial dependence is large enough to be easily measured. Although we have focused on J/ψ , the approach used here should apply to other hard probes such as Υ , W^\pm , Z^0 , Drell-Yan, open heavy flavor and jet production.

We thank K.J. Eskola and V. Guzey for providing the shadowing routines and for discussions. This work was supported in part by the Division of Nuclear Physics of the Office of High Energy and Nuclear Physics of the U. S. Department of Energy under Contract Number DE-AC03-76SF00098.

REFERENCES

- [1] J.J. Aubert *et al.*, Nucl. Phys. **B293**, 740 (1987); M. Arneodo, Phys. Rep. **240**, 301 (1994).
- [2] V. Emel'yanov, A. Khodinov, S.R. Klein and R. Vogt, Phys. Rev. C **61**, 044904 (2000).
- [3] T. Kitagaki *et al.*, Phys. Lett. **B214**, 281 (1988).
- [4] A.D. Frawley *et al.* (PHENIX Collaboration), in proceedings of Quark Matter '02, Nantes, France, July, 2002 [arXiv:nucl-ex/0210013].
- [5] B.L. Combridge, Nucl. Phys. **B151**, 429 (1979).
- [6] R.V. Gavai, D. Kharzeev, H. Satz, G. Schuler, K. Sridhar and R. Vogt, Int. J. Mod. Phys. **A10**, 3043 (1995); G.A. Schuler and R. Vogt, Phys. Lett. **B387**, 181 (1996).
- [7] C.W. deJager, H. deVries, and C. deVries, Atomic Data and Nuclear Data Tables **14**, 485 (1974).
- [8] D. Kharzeev, E. Levin and M. Nardi, hep-ph/0212316; L. Hulthen and M. Sagawara, in *Handbüch der Physik*, **39** (1957).
- [9] A.D. Martin, R.G. Roberts, and W.J. Stirling, and R.S. Thorne, Phys. Lett. **B443**, 301 (1998).
- [10] M. Glück, E. Reya, and A. Vogt, Z. Phys. **C53**, 127 (1992).
- [11] K.J. Eskola, V.J. Kolhinen and P.V. Ruuskanen, Nucl. Phys. **B535**, 351 (1998).
- [12] K.J. Eskola, V.J. Kolhinen and C.A. Salgado, Eur. Phys. J. **C9**, 61 (1999).
- [13] L. Frankfurt, V. Guzey and M. Strikman, arXiv:hep-ph/0303022.
- [14] H.L. Lai *et al.*, Eur. Phys. J. **C12**, 375 (2000).
- [15] A.D. Martin, R.G. Roberts, and W.J. Stirling, and R.S. Thorne, Eur. Phys. J. **C4**, 463 (1998).
- [16] J. Badier *et al.* [NA3 Collaboration], Z. Phys. C **20**, 101 (1983); D.M. Alde *et al.* [E772 Collaboration], Phys. Rev. Lett. **66**, 2285 (1991).
- [17] S. Gavin and M. Gyulassy, Phys. Lett. B **214**, 241 (1988); J.P. Blaizot and J.Y. Ollitrault, Phys. Lett. B **217**, 392 (1989); J. Hufner, Y. Kurihara and H.J. Pirner, Phys. Lett. B **215**, 218 (1988); P. Hoyer and S. Peigne, Phys. Rev. D **57**, 1864 (1998).
- [18] R. Vogt, Phys. Rev. **C61**, 035203 (2000); Nucl. Phys. A **700**, 539 (2002).
- [19] V. Emel'yanov, A. Khodinov, S.R. Klein and R. Vogt, Phys. Rev. **C56**, 2726 (1997).
- [20] V. Emel'yanov, A. Khodinov, S.R. Klein and R. Vogt, Phys. Rev. Lett. **81**, 1801 (1998).
- [21] V. Emel'yanov, A. Khodinov, S.R. Klein and R. Vogt, Phys. Rev. C **59**, R1860 (1999).
- [22] A. L. Ayala, M. B. Gay Ducati and E. M. Levin, Nucl. Phys. **B493**, 305 (1997).
- [23] Z. Huang, H. Jung Lu and I. Sarcevic, Nucl. Phys. **A637**, 79 (1998).
- [24] I. Chemakin *et al.*, Phys. Rev. **C60**, 024902 (1999).
- [25] M. Beddo *et al.*, Nucl. Instrum. & Meth. **A499**, 725 (2003); C. E. Allgower *et al.*, Nucl. Instrum. & Meth. **A499**, 740 (2003).
- [26] ALICE Collaboration, Technical Design Report of the Transition Radiation Detector, LHC/LHCC **2001-021** (2001).
- [27] CMS Collaboration, Technical Proposal, CERN-LHCC-94-38, 1994.
- [28] ALICE Collaboration, Muon Spectrometer Technical Proposal, CERN/LHCC **96-32** (1996); A. Morsch [ALICE Collaboration], Nucl. Phys. A **638**, 571 (1998).

FIGURES

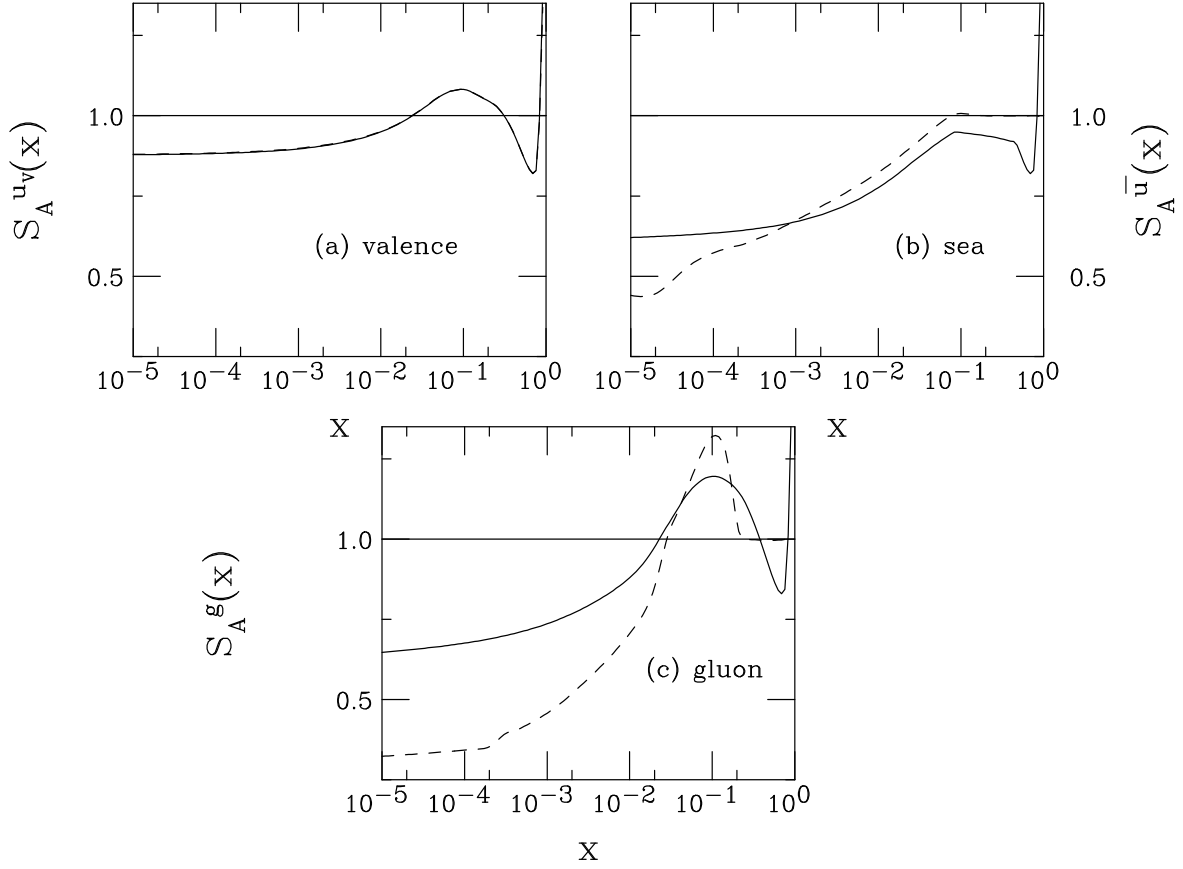


FIG. 1. The EKS98 and FGS shadowing parameterizations are compared at the scale $\mu = 2m_c = 2.4$ GeV. The solid curves are the EKS98 parameterization, the dashed, FGS.

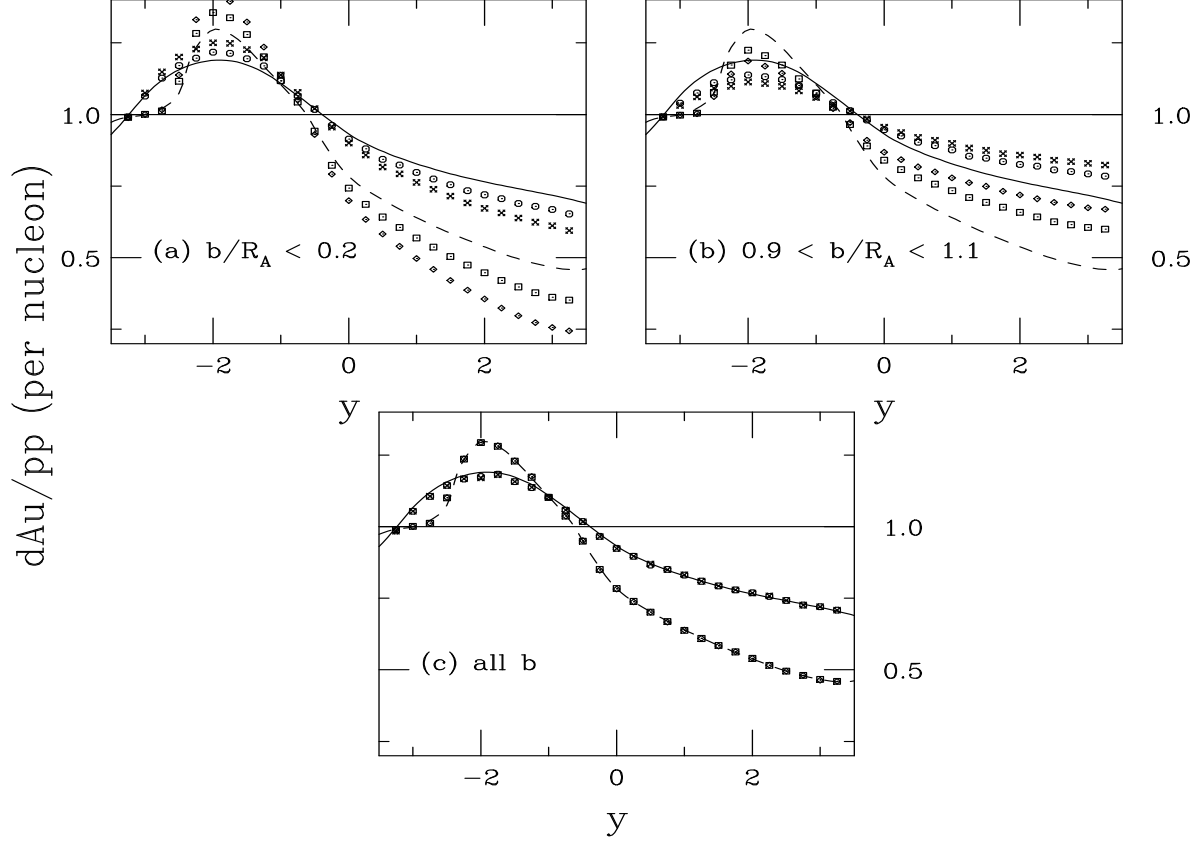


FIG. 2. The J/ψ shadowing ratio at 200 GeV as a function of rapidity. The results are shown for the EKS98 (solid line for homogeneous shadowing, circles and x's for $S_{\text{EKS98,WS}}^i$ and $S_{\text{EKS98},\rho}^i$ respectively) and FGS (dashed line for homogeneous shadowing, squares and diamonds for $S_{\text{FGS,WS}}^i$ and $S_{\text{FGS},\rho}^i$ respectively). The impact parameter bins are (a) $b/R_A < 0.2$, (b) $0.9 < b/2R_A < 1.1$, and (c) all b .

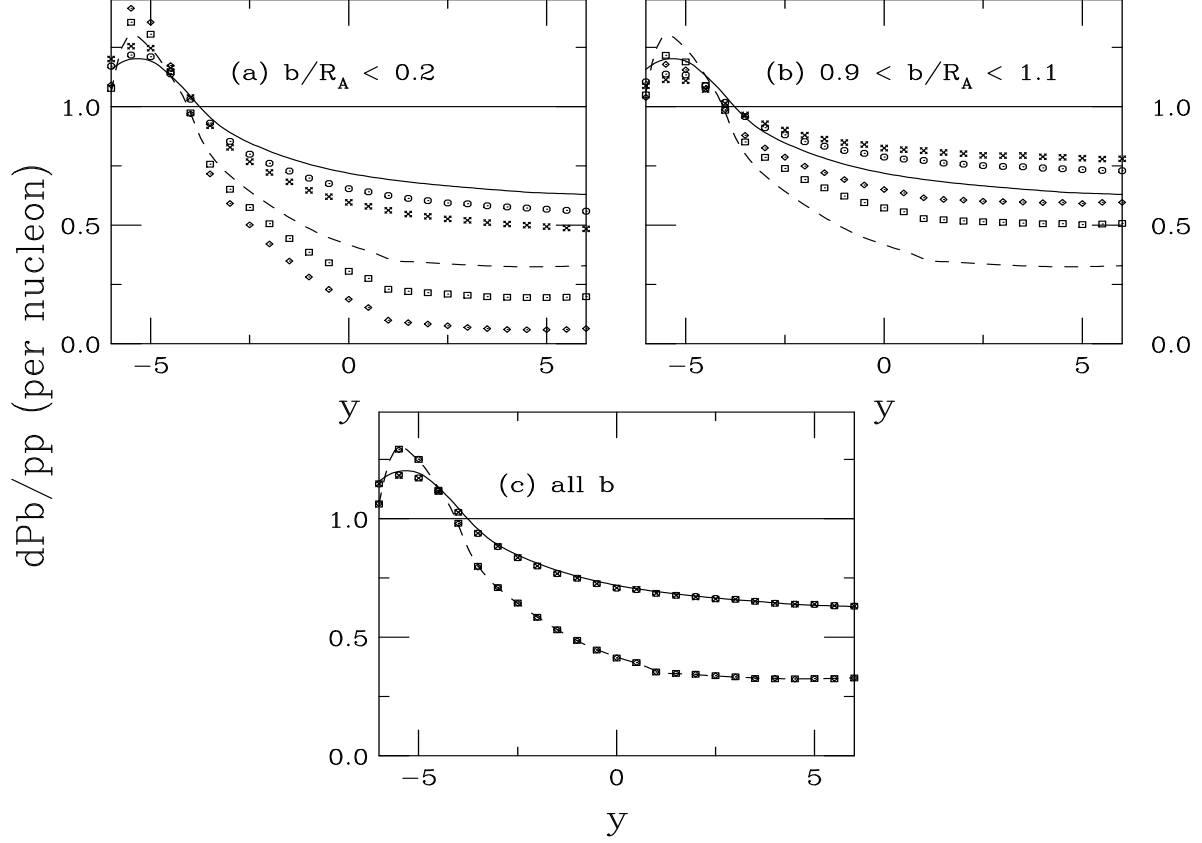


FIG. 3. The J/ψ shadowing ratio at 6.2 TeV as a function of rapidity. The results are shown for the EKS98 (solid line for homogeneous shadowing, circles and x's for $S_{\text{EKS98,WS}}^i$ and $S_{\text{EKS98,\rho}}^i$ respectively) and FGS (dashed line for homogeneous shadowing, squares and diamonds for $S_{\text{FGS,WS}}^i$ and $S_{\text{FGS,\rho}}^i$ respectively). The impact parameter bins are (a) $b/R_A < 0.2$, (b) $0.9 < b/2R_A < 1.1$, and (c) all b .